PCCP

Accepted Manuscript

This is an *Accepted Manuscript*, which has been through the Royal Society of Chemistry peer review process and has been accepted for publication.

Accepted Manuscripts are published online shortly after acceptance, before technical editing, formatting and proof reading. Using this free service, authors can make their results available to the community, in citable form, before we publish the edited article. We will replace this *Accepted Manuscript* with the edited and formatted *Advance Article* as soon as it is available.

You can find more information about *Accepted Manuscripts* in the Information for Authors.

Please note that technical editing may introduce minor changes to the text and/or graphics, which may alter content. The journal's standard Terms & Conditions and the Ethical guidelines still apply. In no event shall the Royal Society of Chemistry be held responsible for any errors or omissions in this *Accepted Manuscript* or any consequences arising from the use of any information it contains.

ROYAL SOCIETY OF CHEMISTRY

www.rsc.org/pccp

Physical Chemistry Chemical Physics RSCPublishing

ARTICLE

Energetic Requirements for Iridium(III) Complex Based Photosensitisers in Photocatalytic Hydrogen Generation†

Cite this: DOI: 10.1039/xoxxoooooox

Received ooth January 2012,
Accepted ooth January 2012

DOI: 10.1039/xoxxoooooox

www.rsc.org/

Shengqiang Fan,[a] Xu Zong,[b] Paul E. Shaw,[a] Xin Wang,[a] Yan Geng,[a] Arthur R. G. Smith,[a] Paul L. Burn,[a] Lianzhou Wang[b] and Shih-Chun Lo,*[a]

A new family of Ir(III) complexes were synthesised and employed as light-induced hydrogen-production photosensitisers in aqueous systems, where hydrogen evolution was only observed when the PS* was reduced by the sacrificial agent, NEt_3, signifying a minimum potential difference of >0.2 V between $E(PS^*/PS^-)$ and $E(NEt_3^+/NEt_3)$ is required for efficient hydrogen production [*i.e.,* $E(PS^*/PS^-)$ >1.19 V *versus* NHE]. The analytical method developed here is demonstrated useful for screening new photosensitisers for light-driven hydrogen generation.

Introduction

Iridium(III) [Ir(III)] complexes with a general structure of $[Ir(C^N)_2(N^N)]^+$ have been developed active photosensitisers (PS) for hydrogen generation from water, in which C^N is a cyclometallating ligand such as 2-phenylpyridine, and N^N is a diimine ligand like 2,2′-bipyridine.[1-3] One of the key advantages for using such Ir(III) heteroleptic structural motifs is that the spatial separation of their highest occupied molecular orbitals (HOMOs) and lowest unoccupied molecular orbitals (LUMOs) enables the independent tuning of the HOMO and LUMO energy levels by manipulating the C^N cyclometallic ligands and/or the N^N co-ligands. Calculations have shown that the HOMO of this type of Ir(III) complex PS is predominantly located on the Ir(III) metal and the C^N ligands, while the LUMO is mainly on the N^N co-ligand.[4] Therefore, the electronic and photophysical properties of these Ir(III) complexes are sensitive to the nature of the C^N and N^N ligands.[5,6] There have been a number of Ir(III) complex PS developed with C^N ligands such as phenylpyridine substituted with halo, alkyl, alkoxy or phenylsilyl moieties to show various hydrogen production activity from aqueous system using a amine type of sacrificial reagent (triethylamine or triethanolamine) and a catalyst like platinum or rhodium. Recently, [Ir(III)] complex photosensitisers based on new C^N ligands such as phenylazole,[7,8] phenylbenzothiazole,[9] and thienylpyridine,[10] containing alternate (to bipyridine) N^N diimine co-ligands including pyridyl triazine and pyrozolyl pyridine were also developed.[11,12] What is clear from these studies is that hydrogen can be generated from the aqueous system but the activity of the PS varied widely. As a consequence, the relationship between the properties of a photosensitiser and hydrogen-generation activity is still not clear. For example, the photophysical properties of the PS such as photoluminescence quantum yields (PLQYs) and lifetime are not straightforwardly related to the photocatalytic activity – a number of Ir(III) complexes having low luminescence and short lifetimes have been found to be active for the photocatalytic hydrogen production.[2,7]

More importantly, the energy requirements for hydrogen generation, which involves charge transfer processes, have not yet been fully established with many studies relying on PL quenching studies.[11] The problem with this approach is that it is difficult to analyse those photosensitisers with weak emission. In order to build our understanding of the effect of PS energy levels on photon-driven catalytic hydrogen production activity and establish the minimum energetic requirements for PS, we report the synthesis and characterisation of a new family of $[Ir(C^N)_2(N^N)]^+$ complexes (**PS2–PS6**, Fig. 1) bearing a range of π-conjugated C^N ligands (**L2–L6**). We evaluate the relative hydrogen-generation performance of the new PS by comparing with the prototypical Ir(III) complex, **PS1**.[1a] From Stern-Volmer measurements and kinetics studies, we confirm that the reduction of the excited state of PS, PS*, by the sacrificial agent is the rate-determining step for the overall hydrogen generation process. We have found that for a PS to be effective in photocatalytic hydrogen generation, there has to be a sufficiently high driving force for PS* to be reduced to PS^{*-} by the sacrificial agent, to enable the subsequent electron transfer from PS^- to the catalyst.

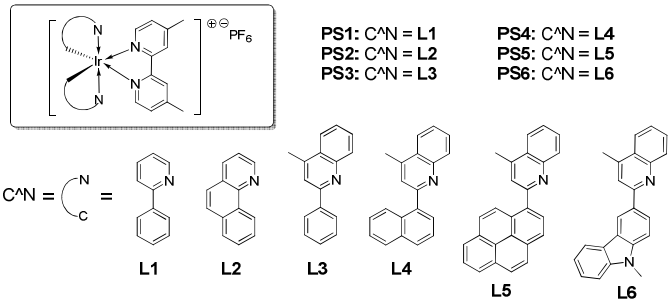

Figure 1. Chemical structures of Ir(III) complexes **PS1**–**PS6** and the respective C^N ligands **L1**–**L6**.

Results and discussion

Synthesis and characterisation. The new family of $[Ir(C^N)_2(N^N)]^+$ complexes, **PS2–PS6**, was synthesised in four

Physical Chemistry Chemical Physics Accepted Manuscript

steps as outlined in Scheme 1, involving ligand synthesis, complexation to form a chloro-bridged iridium(III) dimer, ligation with the N^N co-ligand (*i.e.*, 4,4′-dimethyl-2,2′-bipyridine, dmebpy),[1a,11] and finally counteranion exchange with potassium hexafluoride (KPF_6).[11] While benzo[*h*]quinoline ligand **L2** is commercially available, **L3**–**L6** were first prepared from 2-chloro-4-methylquinoline with the corresponding arylboronic acids under Suzuki-Miyaura cross-coupling reaction conditions (Scheme 1).[13] Under these conditions, **L3**–**L6** were obtained in excellent yields of 80% – 99%%. The first step in the complexes formation involved heating iridium(III) trichloride trihydrate ($IrCl_3{\cdot}3H_2O$) with the corresponding C^N ligands in 2-ethoxyethanol and water under standard cyclometallation conditions[14] to give the respective chloro-bridged Ir(III) dimers in ≈47% – 80% yields. Subsequent co-ligation with the N^N ancillary ligand to form **PS2**–**PS4** was achieved by treating the corresponding Ir(III) dimers with dmebpy in a mixture of dichlomethane and methanol heated at reflux (Method A). We found higher reaction temperatures (Method B) were necessary in the synthesis of more bulky **PS5** and **PS6** due to the more sterically hindered ligands, **L5** and **L6**. Finally, the desired Ir(III) complexes **PS2**–**PS6** bearing a PF_6 counteranion were obtained by an anion exchange process with KPF_6 from the corresponding $[Ir(C^N)_2(N^N)]Cl$ complexes in water.[11] Interestingly, for complete anion exchange, it was found large exces of KPF_6 was required for **PS5** and **PS6**. The overall yields for the last two steps were around 51% – 86% for **PS2**–**PS6**. The obtained mass and NMR spectra of **PS2**–**PS6** were consistent with their structures shown in Scheme 1. Single crystals of **PS3** were grown and showed that the Ir-N bonds of the C^N ligands were *trans* to one another (see Supporting Information).[15] The ^{1}H NMR spectra of **PS3** showed one set of the C^N ligand signals and single signal for the methyl protons attached to the bipyridyl, which was consistent with the *trans* arrangement of Ir-N bonds and observed for all the complexes.

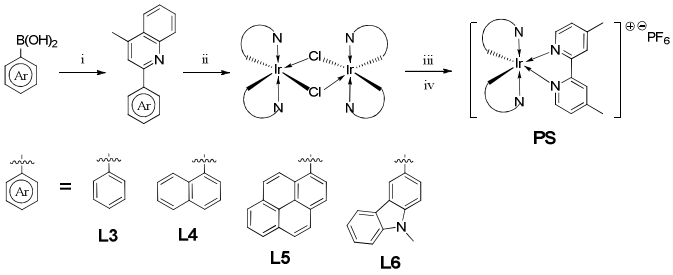

Scheme 1. Synthesis of the Ir(III) complex photosensitisers. Reagents and conditions: (i) 2-chloro-4-methylquinoline, $Pd(PPh_3)_4$, 2 M $Na_2CO_{3(aq)}$, toluene, ethanol, 100 °C, $Ar_{(g)}$. (ii) $IrCl_3{\cdot}3H_2O$, 2-EtOEtOH, water, 120 °C, $Ar_{(g)}$. (iii) Method A (for PS2–PS4): 4,4′-dimethyl-2,2′-bipyridyl, dichlomethane, methanol, 55 °C, $Ar_{(g)}$; or Method B (for PS5 and PS6): 4,4′-dimethyl-2,2′-bipyridyl, ethylene glycol, 150 °C, $Ar_{(g)}$. (iv) KPF_6, water, r.t.

Photophysical properties. The solution UV-visible absorption spectra of the Ir(III) complexes were recorded in dichloromethane at room temperature (Fig. 2), and are compared with that of **PS1**. As can be seen in Fig. 2, the absorption spectra of the new photosensitisers are comprised of three main absorption regions. The intense absorption bands with high molar extinction coefficients (ε) of ≈20,000 – 94,000 $dm^3\ mole^{-1}\ cm^{-1}$ at higher energy (<300 nm for **PS1**–**PS4**, and <440 nm for **PS6**, and <500 nm for **PS5**) consist of the spin-allowed ligand-centred transitions (^{1}LC, *i.e.*, $\pi \rightarrow \pi^*$ transitions of the C^N ligands and N^N ligands).[16] The ligand centred transitions are slightly red-shifted relative to the corresponding free ligands.[17] The weaker absorptions at longer wavelengths (≈380 – 440 nm for **PS2**, ≈380 – 470 nm for **PS3**, ≈420 – 520 nm for **PS4**, ≈480 – 540 nm for **PS5**, and ≈440 – 500 nm for **PS6**) correspond to the singlet inter-ligand charge-transfer (^{1}LLCT) and singlet "metal-to-ligand charge-transfer" transitions (^{1}MLCT) containing $^1MLCT_{C^N}$ and $^1MLCT_{N^N}$ character.[18] Finally, the weak absorptions at longer wavelengths (inset of Fig. 2) can be ascribed as triplet excitations including ^{3}LC, ^{3}LLCT, $^3MLCT_{C^N}$ and $^3MLCT_{N^N}$ transitions.[16,18,19]

As shown in Fig. 2, the absorption characteristics of the Ir(III) complexes are strongly dependent on the C^N ligands. **PS1** and **PS2** have similar onsets to absorption with that of **PS3** being at a slightly longer wavelength, which is due to the extended π-conjugated of the phenylquinoline ligand. By replacing the ligand phenyl ring in **PS3** with a naphthalene or pyrene to give **PS4** and **PS5**, respectively, there is a significant red shift in the onset of absorption, up to ≈600 nm (inset of Fig. 2) for **PS4** and **PS5**. Although **PS6** has carbazole-based ligands, there is only a small red shift in absorption with respect to its parent complex, **PS3** (inset of Fig. 2). Interestingly, the molar extinction coefficient of **PS6** is nearly doubled between 250 and 550 nm (Fig. 2), compared to **PS3**.

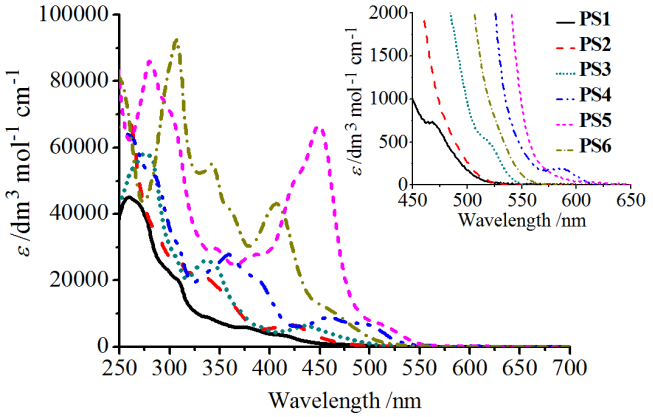

Figure 2. Absorption spectra of the Ir(III) complexes **PS1**–**PS6** in dichloromethane at room temperature [inset: the low energy transitions have been magnified for clarity].

Next, the solution photoluminescence (PL) spectra of **PS1**–**PS6** were measured in deoxygenated dichloromethane at room temperature and are plotted in Fig. 3 with the PL data summarised in Table 1. Upon photoexcitation at 410 nm, all the Ir(III) complexes were luminescent in the visible region with PL peaks in the range of 550 – 624 nm apart from **PS5**, which had a PL peak at 704 nm, and is consistent with the trends observed in the absorption spectra (Fig. 2). Interestingly, the profiles of the PL spectra fall into two different families (Fig. 3). **PS1**, **PS2** and **PS6** have broad featureless profiles while **PS3**–**PS5** have more structured PL spectra with a clear shoulder at longer wavelengths. A broad emission spectrum has been ascribed to transitions with strong ^{3}MLCT character, [*i.e.*, C^N π-orbital and Ir(III) d-orbital to the N^N π^*-orbital), which is mainly due to the presence of the low-lying π^*-orbitals of the diimine ligands],[19b,20] while the more structured PL has been attributed to transitions that have a higher proportion of ^{3}LC character (*i.e.*, $\pi \rightarrow \pi^*$ transitions) in the excited states.[1a,21]

Given the similarity in the onset to the absorption, it is not surprising that **PS1** and **PS2** have similar PL peaks **PS1** (≈580 nm, Fig. 3). What is perhaps surprising is that the PL spectrum of **PS3** is blue shifted relative to **PS1**, although this difference may well arise from the fact that **PS3** has more ^{3}LC character in its emission. As expected in extending the conjugation length of the ligand in moving from **PS3** to **PS4** and **PS5** the emission becomes more red-shifted. In the case of **PS6**, the low energy emission (with a PL peak at 624 nm)

Physical Chemistry Chemical Physics Accepted Manuscript

This journal is © The Royal Society of Chemistry 2012

is similar to that reported for other Ir(III) complexes bearing aryl carbazolyl C^N ligands.[22]

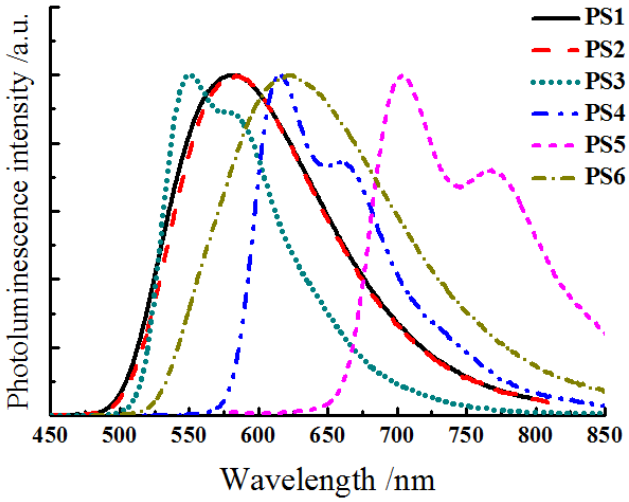

Figure 3. Photoluminescence spectra of Ir(III) complex **PS1**–**PS6** in deoxygenated dichloromethane.

The solution photoluminescence quantum yields (PLQYs) of the Ir(III) complexes were measured in degassed tetrahydrofuran (THF) using a relative method with coumarin 30 as the reference.[25] We measured **PS1** to have a PLQY of 28%, which is comparable to that (31%) reported in dichloromethane.[19b] **PS2** was found to have a similar moderate PLQY (24%) (Table 1), whereas **PS3** and **PS4** with the phenyl and napthylquinoline ligands were found to have higher PLQYs of 80% and 41%, respectively. In contrast, the pyrene and carbazole containing complexes had low PLQYs of 1.4% and 6% for **PS5** and **PS6**, respectively.

Table 1. Photophysical characterisations.

Ir(III) complex	PL peaks[a] /nm	E_g(opt)[b] /eV	PLQYs[c] /%	τ[c] /μs	k_r[d] /×10^5 s^{-1}	k_{nr}[d] /×10^5 s^{-1}
PS1	580	2.45	28 ± 4	0.53	5.3	13.6
PS2	583	2.43	24 ± 3	0.62	3.9	12.3
PS3	550, 578sh	2.34	80 ± 5	2.37	3.4	0.8
PS4	616, 654sh	2.08	41 ± 4	3.34	1.2	1.8
PS5	704, 771sh	1.93	1.4 ± 0.1	3.11	0.045	3.2
PS6	624	2.27	6 ± 2	0.13	4.6	72.3

[a] Measured in dichloromethane. [b] Using the crossover of absorption and emission spectra obtained from diluted dichloromethane.[23] [c] Measured in degassed THF, with excitation at 410 nm. [d] Derived from PLQY = $k_r/(k_r + k_{nr})$ and $\tau = 1/(k_r + k_{nr})$.[24]

The excited-state lifetimes of the Ir(III) complexes were measured in degassed THF with the values summarised in Table 1. The excited state lifetimes were found to be of order a microsecond, reflecting the phosphorescent nature of the emission of the Ir(III) complexes, and are comparable to those of reported for other Ir(III) complexes with 2,2′-bipyridine N^N co-ligands. The excited state lifetimes of the complexes can be divided into two families, namely, those with the longer excited-state lifetimes of 2.4 – 3.3 μs (**PS3**–**PS5**), and those with much shorter PL lifetimes of 0.13 – 0.62 μs (for **PS1**, **PS2** and **PS6**). The longer excited state lifetimes for **PS3**–**PS5** can be attributed to their more significant ^{3}LC character in the emissive state,[26] and are consistent the more structured PL spectra as discussed earlier.

The radiative (k_r) and non-radiative (k_{nr}) rate constants of the complexes were calculated from the PLQY values and excited state lifetimes.[24] While most of the Ir(III) complexes had a typical k_r in the order of 10^5 s^{-1},[19,27] **PS5** had a relatively low k_r (10^3 s^{-1}) due to the higher proportion of ^{3}LC emission arising from the pyrenylquinoline ligands and **PS6** had a slightly larger k_{nr} (7.2×10^6 s^{-1}).

Electrochemical properties. Cyclic voltammetry (CV) was used to investigate the electrochemical behaviour and determine the redox potentials of the complexes. The cyclic voltammetry was carried out on solutions of the complexes in THF using 0.1 M of tetra-*n*-butylammonium hexafluorophosphate (TBAH) as a supporting electrolyte under an argon atmosphere. The cyclic voltammagrams are shown in the Supporting Information (Figures S2–S7) and the $E_{1/2}$s are listed in Table 2 against NHE.[28]

We found that **PS1** had a chemically quasi-reversible oxidation in THF with an $E_{1/2}$(ox) at +1.58 V *versus* the NHE, which is similar to that reported for Ir(ppy)$_2$(bpy)PF$_6$ in acetonitrile (+1.52 V *versus* NHE),[5] **PS3** and **PS4** also exhibited a chemically quasi-reversible oxidation in THF with the $E_{1/2}$(ox)s at +1.57 V and +1.53 V *versus* NHE, respectively. The oxidation $E_{1/2}$ of **PS2**, **PS5** and **PS6** could not be determined in THF but in dichloromethane, a quasi-reversible process for **PS2** and reversible processes for **PS5** and **PS6** were observed with $E_{1/2}$(ox)s of +1.51 V, +1.08 V and +1.24 V *versus* NHE for **PS2**, **PS5** and **PS6**, respectively. The less positive oxidation potentials for **PS5** and **PS6** can be attributed to the C^N ligands consisting of the pyrene moiety and carbazolyl units making the complexes easier to oxidise.[29]

In contrast to oxidation, the Ir(III) complexes all showed several reversible reductions in deoxygenated THF at ambient temperature. The first reduction potentials of all the compounds, **PS1**–**PS6**, were essentially the same at around -1.1 V *versus* the NHE, and are comparable to those of similar Ir(III) complexes bearing with 2,2′-bipyridyl N^N co-ligands. It can, therefore, be deduced that the first reduction corresponds to the reduction of the bipyridyl ligand due to its low-lying π^*-orbitals.[19b,30] Two or more chemically quasi-reversible reductions were also observed at more negative potentials for the Ir(III) complexes (see Table 2 and Supporting Information), which can be attributed to the reductions of the two C^N ligands.

Hydrogen generation. Hydrogen-generation efficiencies of the new PS were evaluated using a similar method reported,[2b,11] where the reaction mechanisms (see below) and the role of sacrificial NEt_3 and hydrogen source had been previous studied.[1c,2b,4] Typically, the test reaction mixtures contained 1.00 μmol of PS, 0.48 μmol of K_2PtCl_4, 2.0 mL of NEt_3,[1d] 2.0 mL of H_2O, and 10 mL of THF unless otherwise stated, and a 150 W Xenon lamp was used as the light source. In this work, the evolved hydrogen was collected in a gas burette, which was further analysed by GC to confirm H_2 formation. The volume

Physical Chemistry Chemical Physics Accepted Manuscript

generated was measured and converted to moles using the ideal gas equation. Turnover numbers (TONs) were calculated by dividing the moles of hydrogen atoms (H) obtained by the moles of PS used [*i.e.*, n(H)/n(PS)].[2b,8]

Table 2. Electrochemical properties of the Ir(III) complex PS.

Ir(III) complex	$E_{1/2}$(ox) /V	$E_{1/2}$(red)[c] /V	E(PS*/PS$^-$)[d] /V
PS1	1.58[a]	-1.13, -2.05, -2.31	+1.31
PS2	1.51[b]	-1.07, -1.75, -2.04	+1.36
PS3	1.57[a]	-1.15, -1.59, -1.89	+1.19
PS4	1.53[a]	-1.13, -1.56, -1.83	+0.95
PS5	1.08[b]	-1.07, -1.26, -1.66, -1.92, -2.11	+0.86
PS6	1.24[b]	-1.15, -1.75, -1.90	+1.12

[a] $E_{1/2}$(ox) *versus* NHE, measured in THF. [b] $E_{1/2}$(ox) *versus* NHE, measured in dichloromethane. [c] $E_{1/2}$(red) *versus* NHE, measured in THF. [d] excited-state reduction potential of PS, *versus* NHE, which was calculated by $E_{1/2}$(red) + E_g(opt),[31] where E_g(opt) is listed in Table 1.

Representative kinetic traces of hydrogen evolution are shown in Fig. 4 and the overall TONs of the photosensitisers are summarised in Table 3. While **PS1–PS3** were found to produce hydrogen, **PS4–PS6** did not show detectable activities despite their relatively high absorption extinction coefficients (Fig. 2) and long excited-state lifetimes (Table 1). The TON of **PS2** was determined to be ≈1,340, which is slightly higher than that of **PS1** under the same conditions. Compared to **PS1** and **PS2**, we found **PS3** displayed a relatively low TON of ≈400. The turnover frequency (TOF) was calculated from the initial 5 minutes of hydrogen formation when the process was in a linear range.[2b,8] **PS1** and **PS2** were found to have similar TOF of 33 and 35 min^{-1}, respectively, while **PS3** was lower (21 min^{-1}).

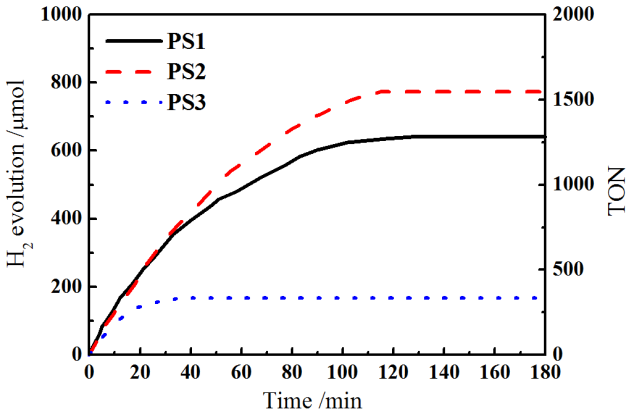

Figure 4. Representative kinetic traces of hydrogen evolution photoreactions with different photosensitisers. Photoreactions contained 1.00 μmol of PS, 0.48 μmol of K_2PtCl_4, 2.0 mL of NEt_3, 2 mL of H_2O, and 10 mL of THF at 20 °C.

Table 3. Results of hydrogen generation.

Ir(III) Complex	$V(H_2)$[a] /mL	$n(H_2)$[a] /μmol	TON[b]	TOF[c] /min^{-1}
PS1	15.4 ± 1.1	641 ± 46	1,281 ± 92	33 ± 2
PS2	16.5 ± 2.3	673 ± 104	1,346 ± 208	35 ± 6
PS3	4.8 ± 0.8	200 ± 33	400 ± 66	21 ± 2
PS4–PS6	-[d]	-[d]	-[d]	-[d]

[a] The reaction mixture contained 1.0 μmol of PS, 0.48 μmol of K_2PtCl_4, 2 mL of triethylamine, 10 mL of THF, and 2 mL of H_2O. [b] n(H)/n(PS).[2b,8] [c] First 5 mins. [d] Not detectable.

Stern-Volmer measurements. To gain insight into the hydrogen-generation activity, Stern-Volmer PL quenching measurements were performed for **PS1–PS6** with triethylamine. The overall Stern-Volmer constants (K_{SV}) were obtained from steady-state Stern-Volmer experiments while the collisional Stern-Volmer constants (K_C) were gained from time-resolved PL measurements.[32] The collisional quenching rate (k_q) values were calculated from $k_q = K_C/\tau_0$, which are tabulated in Table 4.

Table 4. Summary of the Stern-Volmer measurements for **PS1–PS6** at 7 μM in a solvent mixture of THF/H_2O (5:1).

Ir(III) Complex[a]	τ_0[a] /μs	K_{SV}[b](NEt_3) /M^{-1}	K_C[c](NEt_3) /M^{-1}	k_q[d](NEt_3) /×10^6 M^{-1}s^{-1}
PS1	0.33	4.5 ± 0.2	4.1 ± 0.5	12.4 ± 0.4
PS2	0.31	4.2 ± 0.4	3.5 ± 0.4	11.3 ± 0.2
PS3	1.22	0.4 ± 0.2	0.3 ± 0.1	0.3 ± 0.1
PS4–PS6	*no PL quenching was observed*			

[a] τ_0 is the photoluminescence lifetime of the PS in the absence of NEt_3; [b] K_{SV} was obtained from fitting with the steady-state Stern-Volmer equation,[31] $PL_0/PL = 1 + K_{SV}[NEt_3]$, where PL_0 is the initial solution photoluminescence of the PS and PL is the solution photoluminescence of the PS with NEt_3; [c] K_C was obtained from fitting with the time-resolved Stern-Volmer equation,[32] $\tau_0/\tau = 1 + K_C[NEt_3]$, where τ_0 is the initial photoluminescence lifetime of the PS and τ is the photoluminescence lifetime of the PS after addition of NEt_3; [d] k_q was calculated by $k_q = K_C/\tau_0$.

As can be seen in Table 4, **PS2** showed similar K_{SV} and K_C values to **PS1**, which is likely due to their similar C^N ligand structure. However, **PS3** displayed an order of magnitude smaller K_{SV} and K_C values than those of **PS1** and **PS2**, indicating that there was much less PL quenching, and hence a much lower k_q value of 0.3 × 10^6 M^{-1}s^{-1} for **PS3** than **PS2** (11.3 × 10^6 M^{-1}s^{-1}). The PL of **PS4–PS6** was not quenched by NEt_3. Importantly, the quenching process of **PS1-PS3** is predominantly collision in nature.

While the trends in collisional quenching rate are consistent with the hydrogen-generation results (Table 3), the fact that **PS3** has a significant longer excited-state lifetime than **PS1** and **PS2** but exhibits much smaller collisional K_C values would suggest insufficient driving force for electron transfer from NEt_3 to PS*. Hence the performance of **PS3** is limited by the second step in the mechanism proposed by Berhard *et al.*:[2b,4]

(1) $PS \xrightarrow{h\nu} PS^*$

(2) $PS^* + NEt_3 \longrightarrow PS^- + NEt_3^+$ $\quad E_2 = E(PS^*/PS^-) - E(NEt_3^+/NEt_3)$

(3) $PS^- + H^+ \xrightarrow{Pt} PS + 1/2H_2$ $\quad E_3 = E(H^+/H_2) - E(PS/PS^-)$

where E_2 and E_3 are the potential difference of step (2) and (3), respectively; E(PS*/PS$^-$) is the reduction potential of PS in its excited state (*i.e.*, PS*); $E(NEt_3^+/NEt_3)$ is the oxidation potential of NEt_3; $E(H^+/H_2)$ is the hydrogen reduction potential and E(PS/PS$^-$) is the reduction potential of PS. For electron transfer

Physical Chemistry Chemical Physics Accepted Manuscript

This journal is © The Royal Society of Chemistry 2012

to occur in steps 2 and 3, E_2 and E_3 must be greater than zero, meaning that the values of $E(PS^*/PS^-)$ must be larger than $E(NEt_3^+/NEt_3)$, and $E(PS/PS^-)$ must be more negative than $E(H^+/H_2)$. While $E(PS/PS^-)$ corresponds to the first reduction potential of the PS, $E(PS^*/PS^-)$ can not be directly measured. Andreidas *et al.* have estimated $E(PS^*/PS^-)$ from $E(PS/PS^-)$ + E_g(opt),[33] where E_g(opt) is the optical bandgap (Table 1), although it should be noted that the mirror image rule needs to be met for the analysis to be considered valid.

Following the method of Andreidas *et al.*, we estimated the $E(PS^*/PS^-)$ with the data listed in Table 2. Fig. 5 illustrates the energy levels of the photosensitisers against $E(NEt_3^+/NEt_3)$ and $E(H^+/H_2)$.

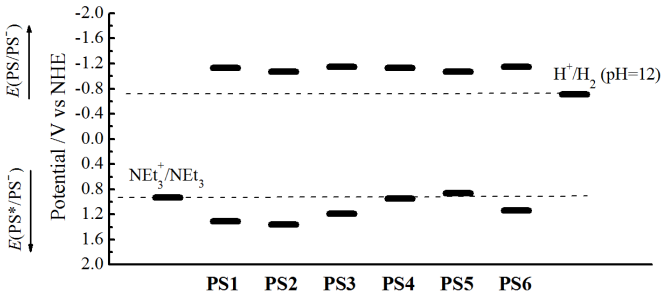

Figure 5. Summary of $E(PS/PS^-)$ of the Ir(III) complex **PS1**–**PS6** *versus* NHE and the calculated $E(PS^*/PS^-)$ by $E(PS/PS^-)$ + E_g(opt).[33]

From Fig. 5, it can be seen that all the PS have more negative $E(PS/PS^-)$ potentials than $E(H^+/H_2)$, indicating that if PS^- were formed for **PS1**–**PS6**, there would be sufficient driving force to accomplish the electron transfer in step 3 of the mechanism. In fact, for the hydrogen-generating complexes, it was found that the performance of the PS was independent of the platinum catalyst concentrations (see Supporting Information, Figure S8), which agrees with the catalyst not being involved in the rate-determining step. In contrast, the new Ir(III) PS have a large variation in the value of $E(PS^*/PS^-)$. The less positive values of $E(PS^*/PS^-)$ for **PS4** and **PS5** are close to that of $E(NEt_3^+/NEt_3)$, and hence step 2 should not occur, which is what was observed in spite of the strong absorption and long excited-state lifetimes (Table 1). For **PS1**–**PS3**, $E(PS^*/PS^-)$ are all more positive than $E(NEt_3^+/NEt_3)$ with the difference ranging from 0.26 – 0.43 V, which again is consistent with Stern-Volmer measurements and these complexes generate hydrogen. In fact, the trend observed in the Stern-Volmer measurements follows the energetics of the system, with the results of the larger Stern-Volmer constant values of **PS1** and **PS2** consistent with the higher driving force for PS* reduction to give PS^- in step 2. In spite of **PS6** having an (E_2) of ≈0.19 V, no hydrogen generation was observed and no PL quenching was measured in the Stern-Volmer measurements. This indicates that an energy difference of <0.2 V is insufficient for triethylamine to generate PS^- from PS* although the role of the short excited state lifetime [it is the shortest of all the complexes in this study (Table 1)] cannot be discounted.

Summary

A new family of Ir(III) complex photosensitisers ligated with π-conjugated cyclometallated ligands and bipyridyl N^N co-ligand were synthesised in excellent yields. High hydrogen-generation TONs of ≈400 – 1,400 were achieved for **PS1**–**PS3** using NEt_3 sacrificial reagent and Pt catalyst. We showed that the rate-determining step in the hydrogen generation is the reduction of the excited photosensitiser. With the current family of materials, it was found that the difference in energy between $E(PS^*/PS^-)$ and $E(NEt_3^+/NEt_3)$ had to be greater than 0.2 V, which is likely to be a general phenomenon for complexes of this type. However, while energetics play a key role in hydrogen generation in some cases the lifetime of the excited state appears to be a second order effect, for example in the case of **PS6**. Thus this work provides a framework for designing and screening efficient photosensitisers for light induced hydrogen generation from aqueous system.

Acknowledgements

We thank Professor Paul V. Bernhardt at the University of Queensland for the single crystal analysis of **PS3**. We acknowledge the financial support from the University of Queensland and Australia Research Council in Discovery Projects. SF thanks the support of an International Postgraduate Research Scholarship (IPRS) from the University of Queensland. Professor Paul Burn is the recipient of University of Queensland Vice Chancellor's Senior Research Fellowship.

Experimental

Materials and general methods. Anhydrous tetrahydrofuran was dried over sodium using benzophenone as an indicator, and distilled immediately prior to use. Thin layer chromatography was performed on Aldrich aluminum plates coated with silica gel 60 P_{254} and visualised with long (365 nm) and short (254 nm) wavelengths UV irradiation. Column chromatography was performed with Merck silica gel (0.063 – 0.200 mm). All solvents used for chromatography were distilled before use. When solvent mixtures are used as eluent, the ratios were given by volume. Kügelrohr distillations were performed using a Büchi B-585 Kügelrohr. ^{1}H and ^{13}C NMR spectra were recorded on Bruker AV300, AV400 and AV500 spectrometers. Chemical shifts are reported in parts per million (ppm) and referenced to the residual solvent peak, *i.e.*, 7.26 ppm for $CDCl_3$ and 2.50 ppm for DMSO-d_6 for the ^{1}H NMR, and 77.0 ppm for $CDCl_3$ and 39.50 ppm for DMSO-d_6 in ^{13}C NMR. Coupling constants, *J*, are reported in hertz (Hz). Peak multiplicities are labeled in the following manner: singlet (s), doublet (d), triplet (t), broad (br), multiplet (m), doublets of doublets (dd), doublets of triplets (dt). ESI mass spectra were recorded on a Bruker HCT 3D Ion Trap using methanol as the solvent and EI mass spectra were recorded on a Finnigan MAT 900 XL. High resolution electrospray ionisation (HRESIMS) accurate mass measurements were carried out on a Bruker MicrOTOF-Q (quadrupole - Time of Flight) instrument with a Bruker ESI source. MALDI-TOF mass spectra were recorded on an Applied Biosystems Voyager MALDI-TOF mass spectrometer using dithranol as the matrix. Elemental microanalyses were carried out using a Carlo Erba NCHS Analyser Model NA 1500 microanalyser at School of Chemistry and Molecular Biosciences, the University of Queensland.

Absorption spectra were recorded on a Varian Cary 5000 UV-Vis-NIR spectrophotometer in spectroscopic grade dichloromethane in 10 × 10 mm quartz cuvettes and λ_{max} values were quoted in nm and shoulders denoted as "sh". Fluorescence spectra were measured using a Jobin-Yvon Horiba Fluorolog in steady-state mode using a xenon lamp as the excitation source. Photoluminescence quantum yields (PLQYs) were determined by using the relative method with coumarin 30 in ethanol (PLQY = 81%), cross-calibrated with quinine sulfate in 0.5 M

Physical Chemistry Chemical Physics Accepted Manuscript

H_2SO_4 (PLQY = 55%), as the reference.[25a] All solutions were prepared in spectroscopic grade tetrahydrofuran in a concentration with an optical intensity of approximately 0.1. Five freeze-pump-thaw cycles were typically employed to degas the solutions. An excitation wavelength of 410 nm was used for the PL measurements. Stern-Volmer measurements were performed by measuring the PL intensity of a degassed PS solution before and after 5 additions of 25 μL of known concentrations of NEt_3. To ensure the concentration of the PS in the cuvette remained constant with each addition the NEt_3 was dissolved in a PS solution with the same concentration as the solution in the cuvette. Furthermore, after each addition of the NEt_3 the mixture was degassed to prevent oxygen quenching. Lifetime measurements were carried out using a Fluorolog 3 with TCSPC capability. The excitation source was an LED emitting at 441 nm and pulsed at 100 KHz with a pulse width of 1.2 ns. The PL was detected at the emission peak of the material and the lifetimes obtained by fitting to the PL decays with single exponentials convolved with the instrument response function.

Cyclic voltammetry (CV) was performed in a standard three-electrode system at room temperature using a solution comprising 1 mM Ir(III) complex and 0.1 M tetra-*n*-butylammonium hexafluorophosphate (TBAH, Fluka, electrochemical grade) as electrolyte in distilled THF or dichloromethane, a glassy carbon working electrode, a Pt wire counter electrode and a $Ag/AgNO_3$ solution as the reference electrode at a scan rate of 100 mV/s. The solutions were purged with argon and measured under an argon atmosphere. Sublimed ferrocene (Fc) was used as a standard and measured under the same conditions as the samples. $E_{1/2}$(ox) and $E_{1/2}$(red) *versus* NHE were calculated using the standard potentials of Fc^+/Fc, ≈0.80 V *versus* NHE in THF and 0.70 V *versus* NHE in dichloromethane.[28]

Hydrogen generation experiments. The hydrogen generation reactions were performed in a triethylamine/photosensitiser/Pt triple-component system.[2] Typically, 1.00 mL of a 1.0 mM photosensitiser stock solution in dichloromethane was added to a 30 mL Schlenk tube and the solvent removed under reduced pressure. Then 10 mL of THF was added to dissolve the photosensitiser with the aid of ultrasonication, followed by the addition of 2 mL of triethylamine and 2 mL of K_2PtCl_4 aqueous solution (2 mg/mL). The reaction solution in the Schlenk tube was then deoxygenated by bubbling with argon for 5 min and then irradiated with a 150 W Xeon lamp (Oriel). The temperature of the reactant solution was maintained at 293±2 K in a transparent water bath. Both the beaker for water bath and the Schlenk tube were made from BOROFLOAT 33 glass in order to filter the UV light (<300 nm) and allow the transmittance of visible light (>325 nm). The H_2 produced was collected in a gas-volume burette and further analysed by gas chromatography (GC-2014, Shimazu).

PS2. A mixture of **L2** (1.00 g, 5.58 mmol), iridium trichloride trihydrate (820 mg, 2.32 mmol), 2-ethoxyethanol (15 mL) and water (5 mL) was heated in an oil bath held at 120 °C under argon for 16 h. The mixture was allowed to cool to room temperature. Water (100 mL) was added to the reaction mixutre to give precipitate. The precipitate was collected by filtration, washed with water (250 mL), methanol (100 mL), and diethyl ether (250 mL), and dried to give the iridium dimer as a red powder (1.14 g, ≈86%), which was used without further purification in the next step. A mixture of the iridium dimer (117 mg, 0.10 mmol), 4,4′-dimethyl-2,2′-bipyridyl (38 mg, 0.21 mmol), dichloromethane (10 mL) and methanol (6 mL) was heated in an oil bath held at 55 °C under argon for 16 h. The mixture was allowed to cool to room temperature and solvents was removed under reduced pressure. A solutiion of KPF_6 (239 mg, 1.30 mmol) in 7 mL of water was added to the mixture, which was manually shaken for 1 minute at room temperature. The formed orange precipitates were then filtered and washed subsequently with distilled water (250 mL) and diethyl ether (250 mL). The precipitate was recrystallised by vapor diffusion of diethyl ether to dichloromethane solution to give **PS2** as an orange solid (90 mg, ≈51%); mp >300 °C (decomp.). λ_{max}(dichloromethane)/nm: 255 (logε/dm^3 mol^{-1} cm^{-1} 4.84), 308 (4.43), 324 (4.36), 421 (3.82), 477sh (2.91). ^{1}H NMR (300 MHz, $CDCl_3$): δ=2.59 (s, 6H), 6.32 (d, J=6.4, 2H), 7.06 (d, J=5.3, 2H), 7.15 (t, J=7.4, 2H), 7.42–7.49 (m, 4H), 7.66 (d, J=8.8, 2H), 7.70 (d, J=5.6, 2H), 7.85 (d, J=8.8, 2H), 7.92 (d, J=4.1, 2H), 8.24 (d, J=8.1, 2H), 8.53 (s, 2H). ^{13}C NMR (100 MHz, DMSO-d_6): δ=20.85, 120.09, 122.74, 124.11, 125.47, 126.65, 128.37, 129.14, 129.45, 129.63, 133.68, 137.47, 140.16, 147.48, 148.44, 149.49, 151.43, 155.38, 156.34. *m/z* [MALDI-TOF]: Anal. Cal. for $C_{38}H_{28}IrN_4$: 731.19 (56%), 732.19 (25%), 733.19 (100%), 734.20 (42%), 735.20 (9%), 736.20 (1%). Found: 731.35 (69%), 732.36 (38%), 733.34 (100%), 734.35 (52%), 735.34 (14%), 736.35 (2%). HRMS (ESI): *m/z* for $[C_{38}H_{28}IrN_4]^+$: 733.1943; found: 733.1933.

PS3. A mixture of **L3**[13a] (1.00 g, 4.56 mmol), iridium trichloride trihydrate (670 mg, 1.90 mmol), 2-ethoxyethanol (30 mL) and water (10 mL) was heated in an oil bath held at 130 °C under argon for 16 h. The reaction was allowed to cool to room temperature. Water (100 mL) was added to the mixture. The resulted precipitate was collected by filtration, washed with water (250 mL), methanol (100 mL), and diethyl ether (250 mL), and dried to give the iridium dimer as a red powder (1.01 g, ≈80%), which was used without further purification in the next step. A mixture of the iridium dimer (133 mg, 0.10 mmol), 4,4′-dimethyl-2,2′-bipyridyl (38 mg, 0.21 mmol), dichloromethane (20 mL) and methanol (6 mL) was heated in an oil bath held at 55 °C under argon for 16 h. The reaction was allowed to cool to room temperature and solvents were removed under reduced pressure. A solutiion of KPF_6 (239 mg, 1.30 mmol) in 7 mL of water was added to the mixture, which was manually shaken for 1 minute at room temperature. The formed orange precipitates were filtered and washed subsequently with distilled water (250 mL), methanol (50 mL) and diethyl ether (250 mL). The precipitate was recrystallised by vapor diffusion of diethyl ether to dichloromethane solution to give **PS3** as an organge solid (165 mg, ≈86%); mp >300 °C (decomp.). λ_{max}(dichloromethane)/nm: 260 (logε/dm^3 mol^{-1} cm^{-1} 4.72), 275 (4.77), 284sh (4.75), 304sh (4.45), 335 (4.42), 365sh (4.14), 388sh (3.79), 435 (3.80), 520sh (2.69). ^{1}H NMR (400 MHz, DMSO-d_6): δ=2.40 (s, 6H), 2.89 (s, 6H), 6.38 (dd, J=7.7 & 0.8, 2H), 6.78 (dt, J=7.6 & 1.2, 2H), 7.06 (dt, J=8.3 & 1.4, 2H), 7.12 (dt, J=8.1 & 1.0, 2H), 7.28 (d, J=8.7, 2H), 7.43 (dt, J=8.1 & 1.0, 2H), 7.51 (dd, J=5.8 & 1.0, 2H), 7.92 (d, J=5.7, 2H), 7.98 (dd, J=8.3 & 1.2, 2H), 8.26 (dd, J=8.1 & 1.0, 2H), 8.34 (s, 2H), 8.47 (s, 2H). ^{13}C NMR (100 MHz, DMSO-d_6): δ=18.45, 20.65, 118.63, 122.38, 124.63, 124.68, 125.60, 126.50, 127.20, 127.32, 128.86, 130.27, 130.43, 133.66, 145.97, 146.34, 146.50, 148.98, 151.32, 151.41, 154.68, 168.83. *m/z* [MALDI-TOF]: Anal. Cal. for $C_{44}H_{36}IrN_4$: 811.25 (55%), 812.26 (28%), 813.26 (100%), 814.26 (48%), 815.26 (12%), 816.26 (2%). Found: 811.37 (52%), 812.38 (34%),

Physical Chemistry Chemical Physics Accepted Manuscript

This journal is © The Royal Society of Chemistry 2012

813.39 (100%), 814.38 (37%), 815.37 (11%), 816.28 (3%). HRMS (ESI): *m/z* for $[C_{44}H_{36}IrN_4]^+$: 813.2569; found: 813.2558. Anal. Cal. for $C_{44}H_{36}F_6IrN_4P$: C, 55.2; H, 3.8; N, 5.9. Found: C, 54.8; H, 3.7; N, 5.9.

PS4. A mixture of **L4**[13b] (606, 2.25 mmol), iridium trichloride trihydrate (330 mg, 0.94 mmol), 2-ethoxyethanol (20 mL) and water (6.5 mL) was heated in an oil bath held at 130 °C under argon for 16 h. The mixture was allowed to cool to room temperature. Water (100 mL) was added to the reaction mixture to give precipitates. The precipitates were collected by filtration, washed with water (250 mL), methanol (50 mL), and diethyl ether (200 mL), and dried to give the iridium dimer as a red powder (532 mg, ≈74%), which was used without further purification in the next step. A mixture of the iridium dimer (153 mg, 0.10 mmol), 4,4′-dimethyl-2,2′-bipyridyl (38 mg, 0.21 mmol), dichloromethane (20 mL) and methanol (6 mL) was heated in an oil bath held at 55 °C under argon for 16 h. The reaction was allowed to cool to room temperature and solvents were removed under reduced pressure. A solutiion of KPF_6 (239 mg, 1.30 mmol) in 7 mL of water was added to the mixture, which was manually shaken for 1 minute at room temperature. The formed orange precipitates were then filtered and washed subsequently with distilled water (250 mL) and diethyl ether (250 mL). The precipitate was recrystallised by vapor diffusion of diethyl ether to dichloromethane solution to give **PS4** as a yellow solid (160 mg, ≈76%); mp >300 °C (decomp.). λ_{max}(dichloromethane)/nm: 255 (logε/dm^3 mol^{-1} cm^{-1} 4.81), 281sh (4.72), 306sh (4.57), 358 (4.44), 384sh (4.33), 458 (3.95), 490 (3.85), 586 (2.32). ^{1}H NMR (400 MHz, DMSO-d_6): δ=2.36 (s, 6H), 2.91 (s, 6H), 6.95 (d, J=8.4, 2H), 7.03 (dt, J=6.8 & 1.3, 2H), 7.33 (dd, J=8.6 & 2.9, 2H), 7.38 (dd, J=5.7 & 0.9, 2H), 7.41–7.49 (m, 4H), 7.66 (dt, J=6.9 & 1.3, 2H), 7.81 (dd, J=8.1 & 0.9, 2H), 7.95 (d, J=5.7, 2H), 7.98 (dd, J=8.3 & 1.1, 2H), 8.17 (s, 2H), 8.60 (s, 2H), 8.76 (d, J=8.7, 2H). ^{13}C NMR (100 MHz, DMSO-d_6): δ=18.74, 20.59, 121.76, 122.36, 123.75, 124.37, 124.49, 125.25, 126.35, 126.36, 127.65, 128.42, 129.70, 130.11, 130.38, 131.08, 131.79, 132.52, 139.14, 146.52, 147.03, 148.22, 151.35, 154.26, 156.61, 170.06. *m/z* [MALDI-TOF]: Anal. Cal. for $C_{52}H_{40}IrN_4$: 911.29 (54%), 912.29 (32%), 913.29 (100%), 914.29 (56%), 915.29 (16%), 916.30 (3%). Found: 911.44 (77%), 912.44 (42%), 913.44 (100%), 914.47 (51%), 915.46 (14%), 916.47 (5%). HRMS (ESI): *m/z* for $[C_{52}H_{40}IrN_4]^+$: 913.2882; found: 913.2881.

PS5. A mixture of **L5** (384 mg, 1.12 mmol), iridium trichloride trihydrate (164 mg, 0.47 mmol), 2-ethoxyethanol (18 mL) and water (6 mL) was heated in an oil bath held at 120 °C under argon for 36 h. The mixture was allowed to cool to room temperature. Water (40 mL) was added to the mixture to give red solid precipitates. The precipitates were filtered, washed thoroughly with water (100 mL), methanol (100 mL) and diethyl ether (250 mL), and dried to give the chloro-bridged iridium dimer as a red solid (200 mg, ≈47%), which was used without further purification in the next step. A mixture of the iridium dimer (148 mg, 0.08 mmol), 4,4′-dimethyl-2,2′-bipyridyl (31 mg, 0.17 mmol), and ethylene glycol (6 mL) was heated in an oil bath held at 150 °C under argon for 20 h. The mixture was allowed to cool to room temperature. Water (50 mL) was added to the reaction mixture. The mixture was extracted with diethyl ether (3 x 30 mL). The ether extracts were combined and the solvent was removed under reduced pressure. A solution of KPF_6 (1.00 g, 5.43 mmol) in 15 mL of water was added to the mixture, which was manually shaken for 1 minute at room temperature. The precipitates formed were filtered and washed subsequently with water (250 mL), a mixture of water/methanol (5:1, 50 mL) and diethyl ether (100 mL). The precipitate was collected and recrystallised by vapor diffusion of diethyl ether to dichloromethane solution to give **PS5** as a red solid (133 mg, ≈55%); mp >300 °C (decomp.). λ_{max}(dichloromethane)/nm: 279 (logε/dm^3 mol^{-1} cm^{-1} 4.94), 295sh (4.87), 345 (4.48), 385sh (4.45), 429sh (4.72), 449 (4.83), 503sh (3.90). ^{1}H NMR (500 MHz, DMSO-d_6): δ=2.34 (s, 6H), 2.98 (s, 6H), 7.05 (dt, J=7.0 & 1.1, 2H), 7.28 (d, J=5.6, 2H), 7.45–7.52 (m, 4H), 7.55 (d, J=8.8, 2H), 7.66 (s, 2H), 7.88 (d, J=9.1, 2H), 7.92 (d, J=5.7, 2H), 7.95 (t, J=7.6, 2H), 8.05 (dd, J=8.4 & 1.0, 2H), 8.13 (t, J=7.6, 2H), 8.15 (s, 2H), 8.28 (d, J=7.6, 2H), 8.34 (d, J=9.5, 2H), 8.76 (s, 2H), 9.07 (d, J=9.5, 2H). ^{13}C NMR (100 MHz, DMSO-d_6): δ=18.82, 20.57, 121.70, 122.61, 123.25, 124.27, 124.43, 125.12, 125.26, 125.28, 125.95, 126.34, 126.63, 126.67, 126.75, 128.33, 129.05, 129.14, 129.60, 129.68, 130.11, 130.62, 131.91, 139.39, 146.92, 147.55, 148.19, 149.22, 151.21, 154.47, 170.11. *m/z* [MALDI-TOF]: Anal. Cal. for $C_{64}H_{44}IrN_4$: 1059.32 (51%), 1060.32 (38%), 1061.32 (100%), 1062.32 (66%), 1063.33 (23%), 1064.33 (6%). Found: 1059.49 (43%), 1060.50 (40%), 1061.49 (100%), 1062.49 (63%), 1063.51 (27%), 1064.49 (15%). HRMS (ESI): *m/z* for $[C_{64}H_{44}IrN_4]^+$: 1061.3190; found: 1061.3196.

PS6. A mixture of **L6** (850 mg, 2.50 mmol), iridium trichloride trihydrate (250 mg, 0.71 mmol), 2-ethoxyethanol (20 mL) and water (6.5 mL) was heated in an oil bath held at 130 °C under argon for 20 h. The mixture was allowed to cool to room temperature. Water (40 mL) was added to the reaction mixture to give red precipitates. The precipitates were filtered, washed thoroughly with water (100 mL), methanol (100 mL) and diethyl ether (250 mL) and dried to give the chloro-bridged iridium dimer as a red solid (400 mg, ≈63%), which was used without further purification in the next step. A mixture of the iridium dimer (174 mg, 0.10 mmol), 4,4′-dimethyl-2,2′-bipyridyl (37 mg, 0.21 mmol), and ethylene glycol (6 mL) was heated under argon in an oil bath held at 150 °C for 20 h. The mixture was allowed to cool to room temperature. Water (50 mL) was added to the reaction mixture. The mixture was extracted with diethyl ether (3 x 30 mL). The ether extracts were combined and the solvent was removed under reduced pressure. A solution of KPF_6 (1.00 g, 5.43 mmol) in 15 mL of water was added to the mixture, which was manually shaken for 1 minute at room temperature. The precipitates formed were filtered and washed subsequently with water (250 mL), a mixture of water:methanol (5:1, 50 mL) and diethyl ether (100 mL). The precipitate was collected and further purified by recrystallisation using vapor diffusion of diethyl ether to the dichloromethane solution to give **PS6** as a red solid (170 mg, ≈73%); mp >300 °C (decomp.). λ_{max}(dichloromethane)/nm: 306 (logε/dm^3 mol^{-1} cm^{-1} 4.97), 341 (4.74), 356sh (4.63), 405 (4.64), 453sh (4.09), 516sh (3.06). ^{1}H NMR (500 MHz, DMSO-d_6): δ=2.39 (s, 6H), 2.94 (s, 6H), 3.17 (s, 6H), 6.46 (s, 2H), 7.00 (dt, J=7.0 & 1.1, 2H), 7.21 (dt, J=6.4 & 1.8, 2H), 7.30-7.43 (m, 8H), 7.46 (d, J=5.1, 2H), 7.98 (t, J=8.5, 4H), 8.21 (d, J=7.7, 2H), 8.31 (s, 2H), 8.66 (s, 2H), 9.19 (s, 2H). ^{13}C NMR (100 MHz, DMSO-d_6): δ=18.55, 20.65, 28.34, 109.20, 112.59, 118.52, 118.60, 119.23, 119.53, 120.54, 123.08, 124.47, 124.67, 125.17, 125.39, 125.76, 126.78, 128.73, 129.88, 137.45, 140.33, 142.50, 146.56, 146.99, 147.81, 149.33, 151.16, 154.80, 169.48. *m/z* [MALDI-TOF]: Anal. Cal.

Physical Chemistry Chemical Physics Accepted Manuscript

for $C_{58}H_{46}IrN_6$: 1017.34 (53%), 1018.34 (35%), 1019.34 (100%), 1020.34 (62%), 1021.35 (20%), 1022.35 (4%). Found: 1017.65 (65%), 1018.67 (34%), 1019.66 (100%), 1020.65 (59%), 1021.67 (24%), 1022.64 (5%). HRMS (ESI): *m/z* for $[C_{58}H_{46}IrN_6]^+$: 1019.3408; found: 1019.3415.

Notes and references

[a]Centre for Organic Photonics & Electronics, The University of Queensland, School of Chemistry and Molecular Biosciences, QLD 4072, Australia.

[b]Nanomaterials Centre, The University of Queensland, School of Chemical Engineering, QLD 4072, Australia.

[*]*E-mail*: s.lo@uq.edu.au

†Electronic Supplementary Information (ESI) available: synthesis and characterisation details of **L5** and **L6**; crystallographic data of **PS3** (CCDC988597); redox CV of **PS1–PS6**; and hydrogen generation kinetics of **PS2**. See DOI: 10.1039/b000000x/

1 a) M. S. Lowry, W. R. Hudson, R. A. Pascal, Jr. and S. Bernhard, *J. Am. Chem. Soc.*, 2004, **126**, 14129; b) M. S. Lowry, J. I. Goldsmith, J. D. Slinker, R. Rohl, R. A. Pascal, Jr., G. G. Malliaras and S. Bernhard, *Chem. Mater.*, 2005, **17**, 5712; c) E. D. Cline, S. E. Adamson and S. Bernhard, *Inorg. Chem.*, 2008, **47**, 10378.

2 a) S. Metz and S. Bernhard, *Chem. Commun.*, 2010, **46**, 7551; b) B. F. Di Salle and S. Bernhard, *J. Am. Chem. Soc.*, 2011, **133**, 11819.

3 C. Wang, K. E. deKrafft and W. Lin, *J. Am. Chem. Soc.*, 2012, **134**, 7211.

4 L. L. Tinker, N. D. McDaniel, P. N. Curtin, C. K. Smith, M. J. Ireland and S. Bernhard, *Chem. Eur. J.*, 2007, **13**, 8726.

5 a) L. L. Tinker and S. Bernhard, *Inorg. Chem.*, 2009, **48**, 10507; b) D. R. Whang, K. Sakai and S. Y. Park, *Angew. Chem. Int. Ed.*, 2013, **5**, 1161.

6 A. R. G. Smith, M. J. Riley, P. L. Burn, I. Gentle, S.-C. Lo and B. Powell, *Inorg. Chem.*, 2012, **51**, 2821.

7 P. N. Curtin, L. L. Tinker, C. M. Burgess, E. D. Cline and S. Bernhard, *Inorg. Chem.*, 2009, **48**, 10498.

8 F. Gärtner, S. Denurra, S. Losse, A. Neubauer, A. Boddien, A. Gopinathan, A. Spannenberg, H. Junge, S. Lochbrunner, M. Blug, S. Hoch, J. Busse, S. Gladiali and M. Beller, *Chem. Eur. J.*, 2012, **18**, 3220.

9 Y.-J. Yuan, J.-Y. Zhang, Z.-T. Yu, J.-Y. Feng, W.-J. Luo, J.-H. Ye and Z.-G. Zou, *Inorg. Chem.*, 2012, **51**, 4123.

10 Y.-J. Yuan, Z.-T. Yu, H.-L. Gao, Z.-G. Zou, C. Zheng and W. Huang, *Chem. Eur. J.*, 2013, **19**, 6340.

11 F. Gärtner, D. Cozzula, S. Losse, A. Boddien, G. Anikumar, H. Junge, T. Schulz, N. Marquet, A. Spannenberg, S. Gladiali and M. Beller, *Chem. Eur. J.*, 2011, **17**, 6998.

12 S. Stagni, S. Colella, A. Palazzi, G. Valenti, S. Zacchini, F. Paolucci, M. Marcaccio, R. Q. Albuquerque and L. De Cola, *Inorg. Chem.*, 2008, **47**, 10509.

13 a) R. Martínez, D. J. Ramón, M. Yus, *Eur. J. Org. Chem.*, 2007, 1599-1605; b) K. R. J. Thomas, M. Velusamy, J. T. Lin, C.-H. Chien, Y.-T. Tao, Y. S. Wen, Y.-H. Hu and P.-T. Chou, *Inorg. Chem.*, 2005, **44**, 5677.

14 a) K. Nonoyama, *Bull. Chem. Soc. Jpn.*, 1974, **47**, 467; b) S. Lamansky, P. Djurovich, D. Murphy, F. Abdel-Razzaq, H.-E. Lee, C. Adachi, P. E. Burrows, S. R. Forrest and M. E. Thompson, *J. Am. Chem. Soc.*, 2001, **123**, 4304; c) S.-C. Lo, E. B. Namdas, P. L. Burn and I. D. W. Samuel, *Macromolecules*, 2003, **36**, 9721.

15 CCDC988597 (**PS3**) contains the supplementary crystallographic data for this paper. These data can be obtained free of charge from The Cambridge Crystallographic Data Centre *via* www.ccdc.cam.ac.uk/data_request/cif.

16 S. I. Bokarev, O. S. Bokareva and O. Kühn, *J. Chem. Phys.*, 2012, **136**, 214305.

17 F. Spaenig, J.-H. Olivier, V. Prusakova, P. Retailleau, R. Ziessel and F. N. Castellano, *Inorg. Chem.*, 2011, **50**, 10859.

18 S.-H. Wu, J.-W. Ling, S.-H. Lai, M.-J. Huang, C. H. Chen and I.-C. Chen, *J. Phys. Chem. A*, 2010, **114**, 10339.

19 a) F. Kessler, R. D. Costa, D. D. Cesnso, R. Scopelliti, E. Ortí, H. J. Bolink, S. Meier, W. Sarfert, M. Grätzel, M. K. Nazeeruddin and E. Baranoff, *Dalton Trans.*, 2012, **41**, 180; b) M. Lepeltier, T. K.-M. Lee, K. K.-W. Lo, L. Toupet, H. L. Bozec and V. Guerchais, *Eur. J. Inorg. Chem.*, 2005, 110.

20 S. Okada, K. Okinaka, H. Iwawaki, M. Furugori, M. Hashimoto, T. Mukaide, J. Kamatani, S. Igawa, A. Tsuboyama, T. Takiguchi and K. Ueno, *Dalton Trans.*, 2005, **9**, 1583.

21 H. J. Bolink, E. Coronado, R. D. Costa, N. Lardiés and E. Ortí, *Inorg. Chem.*, 2008, **47**, 9149.

22 C.-L. Ho, W.-Y. Wong, Z.-Q. Gao, C.-H. Chen, K.-W. Cheah, B. Yao, Z. Xie, Q. Wang, D. Ma, L. Wang, X.-M. Yu, H.-S. Kwok and Z. Lin, *Adv. Funct. Mater.*, 2008, **18**, 319.

23 J. R. Lakowicz, *Principles of Fluorescence Spectroscopy*, 3rd Ed., Springer, New York, 2010.

24 S.-C. Lo, C. P. Shipley, R. N. Bera, R. E. Harding, A. R. Cowley, P. L. Burn and I. D. W. Samuel, *Chem. Mater.*, 2006, **18**, 5119.

25 a) J. N. Demas and G. A. J. Crosby, *J. Phys. Chem.*, 1971, **75**, 991; b) $Ir(ppy)_2(bpy)PF_6$, which is similar to **PS1**, has been reported to have a solution PLQY of 7.07±0.39% when $Ir(ppy)_2(bpy)Cl$ (PLQY = 6.22%) was used as the reference material (Ref. 1a). Underestimation of the PLQY of iridium(III) complexes can occur if the solutions are insufficiently deoxygenated.

26 a) H. Yersina, *Proceedings of SPIE*, 2004, **5214**, 124; b) J. Li, P. I. Djurovich, B. D. Alleyne, M. Yousufuddin, N. N. Ho, J. C. Thomas, J. C. Peters, R. Bau and M. E. Thompson, *Inorg. Chem.*, 2005, **44**, 1713.

27 C. Dragonetti, L. Falciola, P. Mussini, S. Righetto, D. Roberto, R. Ugo and A. Valore, *Inorg. Chem.*, 2007, **46**, 8533.

28 N. G. Connelly and W. E. Geiger, *Chem. Rev.*, 1996, **96**, 877.

29 a) T. Tsuzuki, N. Shirasawa, T. Suzuki and S. Tokito, *Jpn. J. Appl. Phys.*, 2005, **44**, 4151; b) S.-C. Lo, T. D. Anthopoulos, C. P. Shipley, E. B. Namdas, I. D. W. Samuel and P. L. Burn, *Org. Electron.*, 2006, **7**, 85; c) S.-C. Lo and P. L. Burn, *Chem. Rev.*, 2007, **107**, 1097; d) K. A. Knights, S. G. Stevenson, C. P. Shipley, S.-C. Lo, S. Olsen, R. E. Harding, S. Gambino, P. L. Burn and I. D. W. Samuel, *J. Mater. Chem.*, 2008, **18**, 2121.

30 a) F. Neve, A. Crispini, S. Campagna and S. Serroni, *Inorg. Chem.*, 1999, **38**, 2250; b) K. K.-W. Lo, C.-K. Chung, T. K.-M. Lee, L.-H. Lui, K. H.-K. Tsang and N. Zhu, *Inorg. Chem.*, 2003, **42**, 6886; c) Q. Zhao, F. Li, S. Liu, M. Yu, Z. Liu, T. Yi and C. Huang, *Inorg. Chem.*, 2008, **47**, 9256.

31 E. S. Andreiadis, M. Chavarot-Kerlidou, M. Fontecave and V. Artero, *Photochem. Photobiol.*, 2011, **87**, 946.

32 D. A. Olley, E. J. Wren, G. Vamvounis, M. J. Fernee, X. Wang, P. L. Burn, P. Meredith and P. E. Shaw, *Chem. Mater.*, 2011, **23**, 789.

33 E. S. Andreiadis, M. Chavarot-Kerlidou, M. Fontecave and V. Artero, *Photochem. Photobiol.*, 2011, **87**, 946.

Physical Chemistry Chemical Physics Accepted Manuscript

 This journal is © The Royal Society of Chemistry 2012